VRHI: Visibility Restoration for Hazy Images Using a Haze Density Model

Mingye Ju[1], Chuheng Chen[1], Juping Liu[2], Kai Cheng[1], Dengyin Zhang[1*]
[1] Nanjing University of Posts and Telecommunications [2] Macquarie University

Abstract

In this paper, a image processing method called VRHI is developed to enhance single hazy images. More specifically, inspired by visual characteristics of haze, a haze density estimation model is designed to predict the haze distribution. According to this recognized haze distribution, a quadtree based recursive strategy is subsequently proposed to locate the atmospheric light. Finally, by combining a global-wise adjusting mechanism and atmospheric scattering model, the haze cover in an image can be easily excluded using the estimated parameters. It is worth mentioning that VRHI is based on whole image to search the unknown parameters, thereby avoiding some unfavorable phenomena, e.g., over-enhancement and color distortion. Extensive experiments on real-world images and well-known dehazing datasets show that VRHI outperforms state-of-the-art techniques in robustness and effectiveness.

1. Introduction

Due to particles suspended in the air, haze is a common atmospheric phenomenon in daily life. In such condition, the light of the objects would be scattered and absorbed by these particles, which makes the captured images suffer from low visibility and poor contrast. Unfortunately, such low-quality images can not provide the enough information many vision applications to perform subsequent high-level processing [19, 43]. Therefore, a simple and effective image haze removal is becoming an increasingly desirable technique for both computational photography and computer vision systems.

Recently, significant progress has been achieved in image dehazing field. Numerous emerging image haze removal techniques can be mainly classified into two groups: prior-wise methods and learning-wise ones.

Prior-wise methods: The core idea of this type of method is to achieve haze removal by imposing some potential priors on atmospheric scattering model (ASM). For example, Tan [48] realized haze removal by compensating the contrast loss for hazy images. In [15], dark channel prior (DCP) based dehazing approach was proposed by He et al., which reveals at least one channel in natural haze-free patches exists some pixels whose intensities are similar to zero. Using a color attenuation prior, a linear model on the scene depth was designed by Zhu et al. to estimate the transmission of hazy images in [56]. Likewise, based on the fact that a haze-free image is composed of repeated patches [1] or approximated colors [2], [3] , some non-local recovery strategies were developed to obtain a promising recovery performance. Besides, some other approaches [7, 50, 22, 30, 5, 25, 53, 24, 17, 16, 14, 52, 23, 42, 20, 51, 21] also utilized the prior knowledge to achieve the purpose of haze removal.

Learning-wise methods: With the sharp development of machine learning, data-driven manner has attracted significant attention and great success on haze removal has been reached over the past few years. Their core idea is to build the models or networks by learning the latent features from some well-known datasets and then utilize the trained models to remove the haze cover in an image. Depending on the difference of using deep network, learning-wise methods can be further classified into convolutional neural network (CNN) based and generative adversarial network (GAN) based approaches.

CNN-based Approach: Benefitting from the capability of convolutional neural network (CNN) to extract the features, several CNN-based dehazing methods [6, 26, 47, 32, 31, 28, 49, 54, 40, 12, 45, 8, 44] have been proposed recently. For example, a CNN-based system used to estimate transmission map was designed by Cai et al. [6]. Ren et al. [41] created a multi-scale network by learning effective features to achieve a more accurate transmission map. In [26], all-in-one dehazing network (AOD-Net) was proposed to directly obtain the dehazed image from a hazy image via a light-weight CNN. A ranking CNN network was developed in [47] by making an extension of the structure of CNN to make sure that the statistical properties of hazy images can be captured simultaneously. According to some potential priors, Liu et al. [32] established an iteration algorithm using deep CNNs. To obtain a better performance, a trainable CNN named GridDehazeNet [31] was proposed, which is composed of preprocessing, backbone, and post-

*Corresponding author: zhangdy@njupt.edu.cn

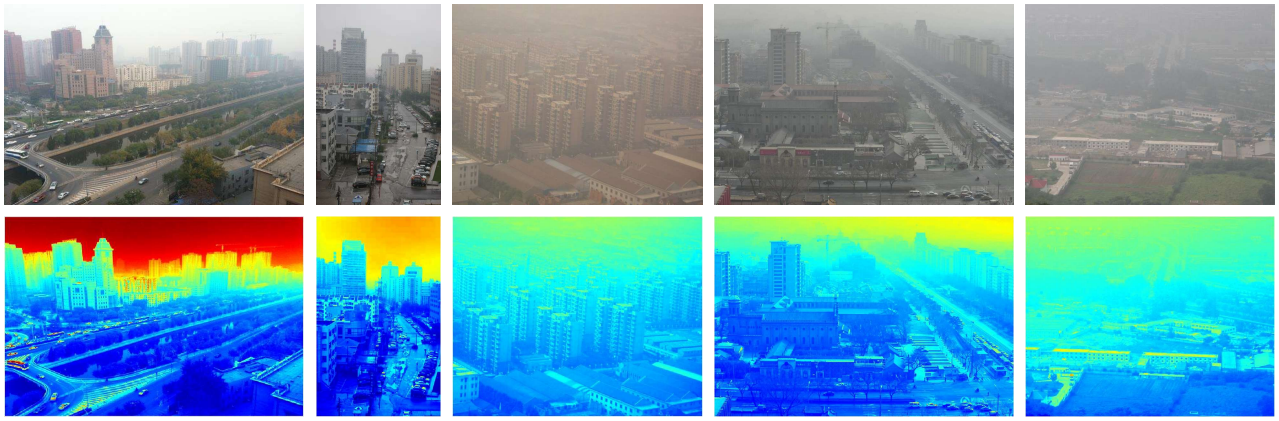

Figure 1. Haze map calculated by Eq. (4) on different hazy images.

processing modules.

GAN-based Approach: In addition to CNN, generative adversarial network (GAN) has also been successfully employed in image dehazing [39, 13, 33, 29, 11, 10, 37, 35, 46, 18, 4, 55, 29]. Typically, some GAN-based architectures [39, 13, 33] have been directly constructed to obtain image-to-image mapping. RI-GAN [10] proposed by Dudhane et al. extended GAN to obtain an accurate transmission estimation. In [46], DHGAN, which is able to capture more global features from the training datasets, was created to improve image dehazing result. In [37], a heterogeneous GAN and a conditional GAN was proposed to restore hazy images and enhance textual details.

Different from current available algorithms, we propose a hazy image restoration technique called VRHI to simultaneously dehaze and diminish the negative effects of adverse atmospheric conditions. It mainly contains the following three contributions:

• We devise a haze distribution estimation model demonstrated as an exponential form, where several dimensions are considered to make a more accurate estimation. Through series of experiments, the obtained results were verified to align with human intuition.

• We employ a recursive quadtree strategy to locate the atmospheric light. To achieve a more reliable result, a normalization post-process is utilized to optimize the rough atmospheric light.

• Relying on the designed haze density model, the initial transmission is derived on a pixel-by-pixel basis and further optimized via a global-wise strategy.

2. Background

The dehazing technique proposed in this work is also based on the well-known atmospheric scattering model (ASM). Formally, this model can be expressed as:

$$\boldsymbol{I}(x,y) = \boldsymbol{A} \cdot \boldsymbol{\rho}(x,y) \cdot t(x,y) + \boldsymbol{A} \cdot (1 - t(x,y)), \quad (1)$$

where $\boldsymbol{I}$ indicates the input hazy image, $\boldsymbol{A}$ is the global atmospheric light that can be used to restore the color tone as well as adjusting the brightness of scene radiance, $\boldsymbol{\rho}$ is the expected restored image, and t is the medium transmission. When the atmospheric particle distribution is homogeneous, the transmission t can be detailed by

$$t(x,y) = e^{-\beta \cdot d(x,y)}, \quad (2)$$

where d is the distance between the target scene and the camera, β is the scattering coefficient. As can be concluded from Eq. (1), haze removal of using ASM is naturally an ill-posed problem due to two unknown parameters in ASM, i.e., atmospheric light $\boldsymbol{A}$ and transmission t.

3. Proposed VRHI

In this section, a simple but effective ASM-based image processing technique named VRHI is developed to enhance single hazy images. It can simultaneously dehaze and diminish the negative effects of adverse atmospheric conditions. Only three modules are included in VRHI, which are hazy density model, atmospheric light location, and global transmission estimation.

3.1. Haze Density Model

In general, the haze density is positively correlated with the minimum channel and the difference between minimum and maximum channel [38]. After repeating experiments, we observe that exponential function can well grasp this relationship as:

$$D(x,y) = I_{min}(x,y) \cdot e^{I_{max}(x,y) - I_{min}(x,y)}, \quad (3)$$

where D is the haze distribution of a hazy image, $I_{min}(x,y) = min_{c \in \{r,g,b\}} I^c(x,y)$, and $I_{max}(x,y) = max_{c \in \{r,g,b\}} I^c(x,y)$. Note that another fact, i.e., haze usually makes a pixel brighter, is also needed to be considered

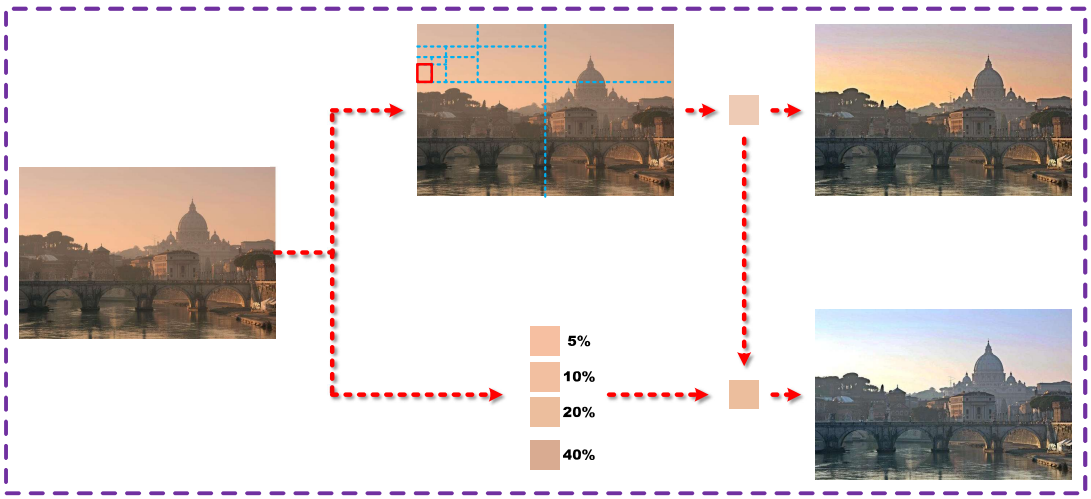

Figure 2. Atmospheric light estimation process.

in Eq. (3). Therefore, we make a more accurate expression for haze density D, i.e.,

$$D(x,y) = I_{min}(x,y) \cdot e^{I_{max}(x,y) - I_{min}(x,y) + \bar{I}(x,y)}, \quad (4)$$

where $\bar{I}(x,y) = \frac{I^r(x,y)+I^g(x,y)+I^b(x,y)}{3}$. Several examples of the calculated haze density map are shown in Fig. 1. It can be illustrated from this figure that the obtained haze density maps are very consistent with the objective laws of real-world.

3.2. Atmospheric Light Location

Relying on the previously estimated distribution, a recursive quad-tree atmospheric light estimation strategy is provided. Unlike the existing quad-tree location approaches [36], our strategy is to adaptively select a pixel point instead of fixing center of an image as the split center. Formally, based on the fact that the atmospheric light is more likely to be in upper part of an image, in each splitting operation, the location of quarter point is selected by

$$(Loc_x, Loc_y) = (\frac{1}{2}\cdot M_x + \frac{1}{2}\cdot N_x, \frac{\gamma-1}{\gamma}\cdot M_y + \frac{1}{\gamma}\cdot N_y), \quad (5)$$

where $\gamma = 3$ is centrifugation parameter, M and N indicates the top left vertex and the bottom right vertex of the current partitioned region respectively, whose coordinates are (M_x, M_y) and (N_x, N_y), (Loc_x, Loc_y) is the coordinate of the quarter point. The first partitioned region is the whole initial image, whose (M_x, M_y) is $(0,0)$ and (N_x, N_y) is (w,h), where w and h is the width and height of an image. The location of the quarter point will determine the boundaries of four new partitioned regions. The average value of the final partitioned region in each channel will be regarded as A^c_{rough}.

This strategy is feasible for most hazy images, unfortunately, it will lose efficacy in addressing images with slight color distortion, since the $\boldsymbol{A}_{rough}$ obtained from a local region may fail to match the whole image. To this end, we calculate the average pixel value of 5%, 10%, 20%, 40% brightest pixels (i.e., $\boldsymbol{A}_{5\%}$, $\boldsymbol{A}_{10\%}$, $\boldsymbol{A}_{20\%}$, $\boldsymbol{A}_{40\%}$) and use them to balance

$$\boldsymbol{A}_f = \frac{\boldsymbol{A}_{rough} + \boldsymbol{A}_{5\%} + \boldsymbol{A}_{10\%} + \boldsymbol{A}_{20\%} + \boldsymbol{A}_{40\%}}{5}, \quad (6)$$

where $\boldsymbol{A}_f$ is the final estimated result atmospheric light. For clarity, the whole process of atmospheric light estimation is illustrated as Fig. 2.

3.3. Global Transmission Estimation

Inspired by [38], we assume that there is an inverse correlation between haze density and transmission map. Accordingly, the transmission t is modeled as:

$$t(x,y) = 1 - f \cdot D(x,y), \quad (7)$$

where f is a fitting coefficient used to preserve a certain amount of haze in recovery result. Note that the haze in the upper part of hazy input is bound to be denser than that in the lower part, thus we introduce a coefficient λ into the Eq. (7) to revise the expression:

$$\lambda(x,y) = e^{-\frac{y}{h}} + 2\cdot(\frac{y}{h} - (\frac{y}{h})^2) + 1, \quad (8)$$

where h is the height of input image. Substituting Eqs. (7) (8) and the estimated $\boldsymbol{A}_f$ into Eq. (1), the scene albedo can be restored as

$$\rho^c(x,y) = \phi(\boldsymbol{I}, \boldsymbol{A}, D, x, y) = \frac{I^c(x,y) - A^c}{A^c \cdot (1 - f \cdot (e^{-\frac{y}{h}} + 2\cdot(\frac{y}{h} - (\frac{y}{h})^2) + 1) \cdot D(x,y))} + 1, \quad (9)$$

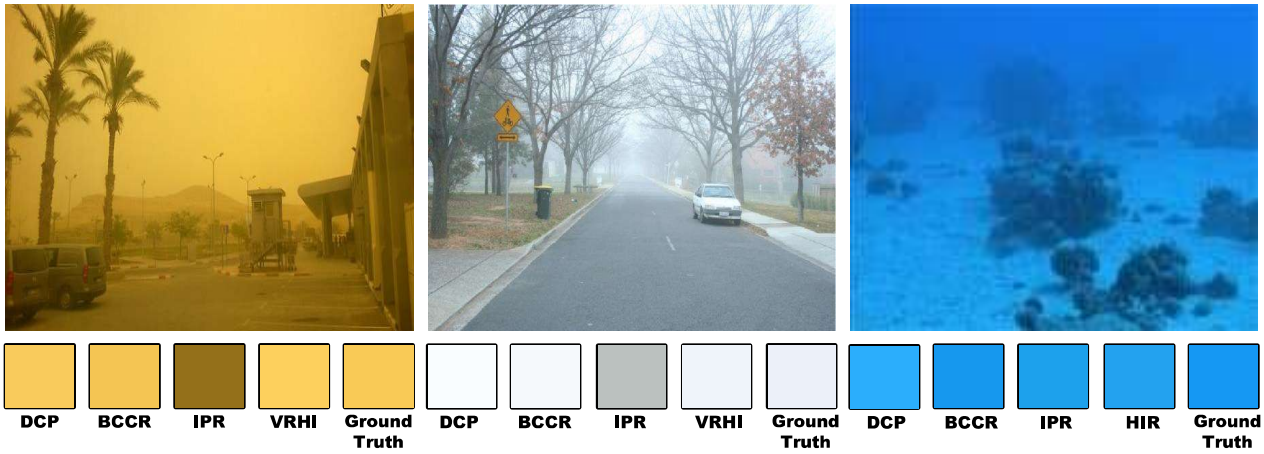

Figure 3. Accuracy for atmospheric light

where $\phi(\cdot)$ is an abbreviation of Eq. (9). Note that only f is unknown parameter in above equation, thus we can search the f by imposing a prior on it, whose procedure can be detailed as

$$f = argmin\{\Psi(\phi(\boldsymbol{I}, \boldsymbol{A}, D, x, y))\}, \tag{10}$$

where $\Psi(\cdot)$ is a function used to maximize the contrast of an input. Once f has been determined, the dehazed result can be easily obtained using Eq. (9).

4. Experiment

In this section, a series of experiments were conducted to test the dehazing performance of VRHI. All the experiments were implemented in MATLAB2020a on a PC with an Intel(R) Core (TM) i5-8265U CPU @ 1.6GHz 8.00 GB RAM. The hazy images used in the experiments were selected from real-world or publicly available datasets.

4.1. Accuracy for Atmospheric Light

Different from other atmospheric light estimation algorithms, the proposed VRHI recursively adjusts $\boldsymbol{A}$ based on the whole image instead of obtaining $\boldsymbol{A}$ from a single pixel, thereby getting a more promising estimation result. To prove it, we selected three representative images to compare our searched atmospheric light and the results obtained by other state-of-the-art techniques, including DCP [15], BCCR [34], IPR [1]. The experimental results together with corresponding ground truth results are illustrated in Fig. 3. It is can be observed from the results that VRHI is capable of estimating the most accurate $\boldsymbol{A}$ compared to others.

4.2. Robustness Test

A reliable dehazing methods should has the ability to process hazy images with different environments. Therefore, we selected images with different haze concentration, varying degrees of color confusion, different scene backgrounds, and various levels of brightness disorder, to test the robustness of VRHI, as shown in Fig. 4. It can be found from this figure that VRHI is able to get rid of negative visual effects, e.g., color distortion and poor contrast, and restore the details of the image fully. Moreover, the estimated transmission map is also verified to align with our intuition.

4.3. Qualitative Comparison on Real-world Images

In this subsection, the five real-world images with different haze levels were picked up to facilitate the comparison between VRHI and state-of-the-art techniques, including EPDN [39], MSBDN [9], DEFADE [7], MSCNN [41], NLD [2]. The selected five images and the recovered images of different techniques are demonstrated in Fig. 5.

It is observed from Fig. 5(b) that EPDN can unveil the contour of the object in the bright regions, but the dark regions seem to be over-saturated. In Fig. 5(c), although MSBDN is able to avoid the problem of over-saturation to some extent, haze will still be found in the recovery results, and the entire image tends to be brighter. DEFADE is able to identify bright areas and enhance the details of most of the hazy samples. Unfortunately, as shown in Fig. 5(d), due to some inherent disadvantages of multi-scale fusion, DEFADE may lose its utility when processing the dark areas of the image. MSCNN is able to achieve satisfactory dehazing performance for some mist images. However, when processing the dense haze image in Fig. 5(e), MSCNN cannot provide an ideal restored haze-free image. It is attributed to the fact that the performance of learning-wise algorithms is usually limited by the intrinsic drawbacks of artificially synthesized images. As shown in Fig. 5(f), NLD obtains visually satisfactory results for most given images. Unfortunately, the restored image tends to become darker due to the limitation of the used prior. Compared with these meth-

Figure 4. Robustness test of VRHI on different hazy images. (a): Hazy Images. (b): Transmission Maps. (c):Results Enhanced by Proposed VRHI.

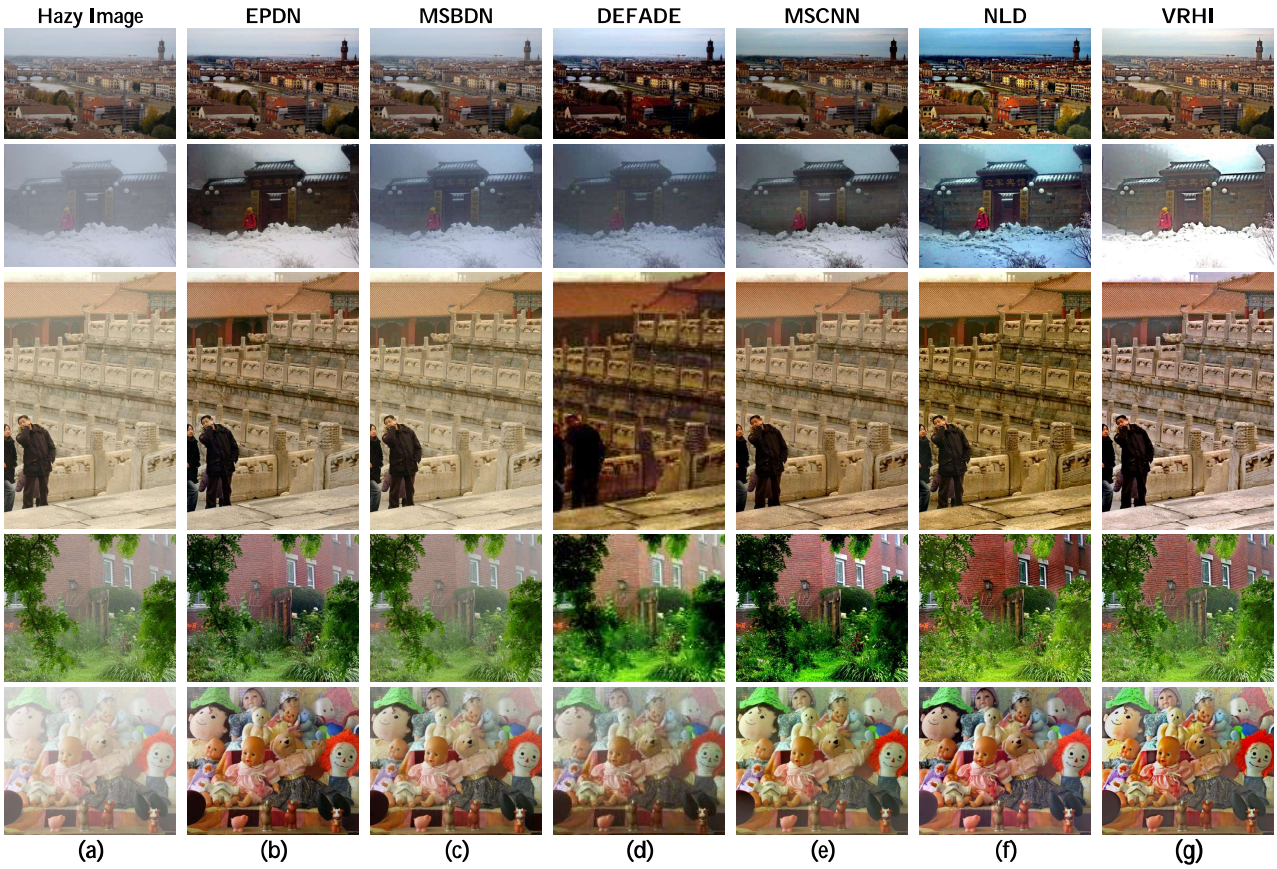

Figure 5. Qualitative comparison between the proposed VRHI and the state-of-the-art techniques on challenging real-world images. (a): Hazy images. (b): EPDN. (c): MSBDN. (d): DEFADE. (e): MSCNN. (f): NLD. (g): VRHI.

ods, VRHI can restore details and improve image quality. As displayed in Fig. 5(g), the images restored by VRHI have no over-saturation, over-enhancement or halo effects, and the recovered color remains natural and the blur areas are enhanced clearly.

Apart from the real-world images, we also used one of most representative synthetic datasets, namely Synthetic Objective Testing Set (SOTS) [27], to test the performance of our VRHI and state-of-the-art dehazing techniques. The synthetic images and the restored results are illustrated in Fig. 6. It can be observed in Fig. 6(b) that dehazed results by EPDN is darker than the ground-truth in some cases. The dehazed images by MSBDN is similar to the ground truth, however, some images in Fig. 6(c) tends to be haze residue. As demonstrated in Fig. 6(d), DEFADE can improve the visual perception quality to some extent, however,

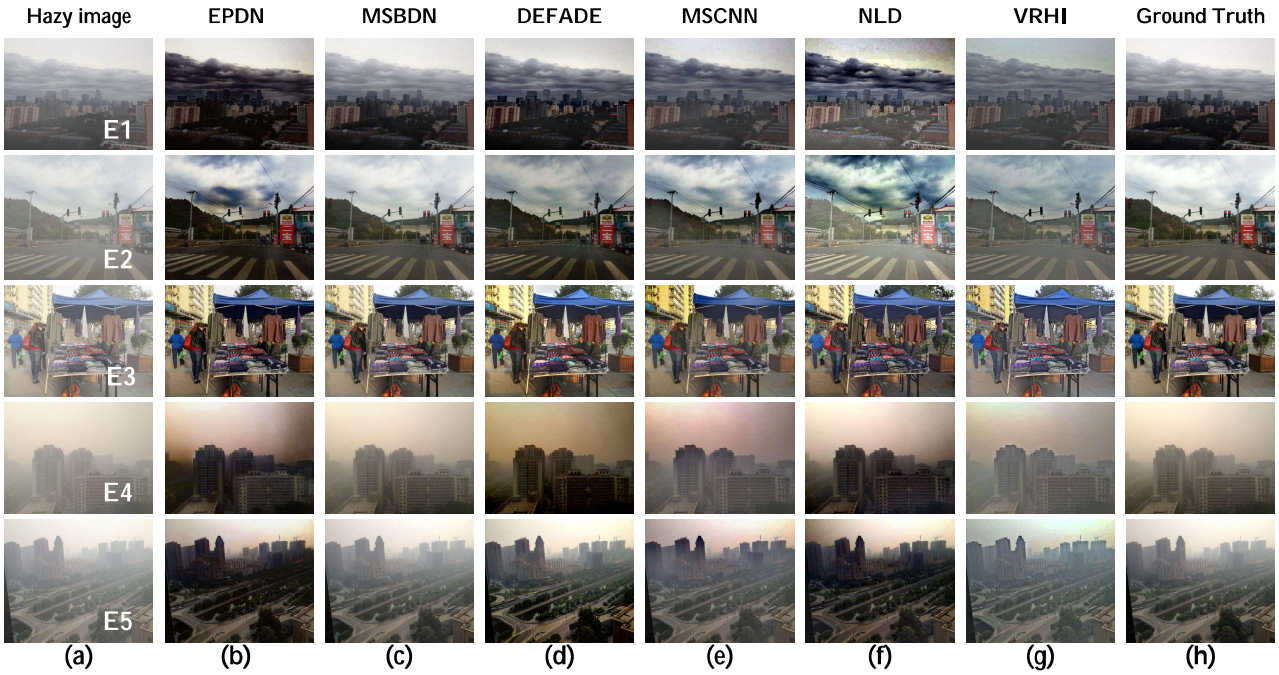

Figure 6. Qualitative comparison between the proposed VRHI and the state-of-the-art techniques on challenging synthetic images. (a): Hazy images. (b): EPDN. (c): MSBDN. (d): DEFADE. (e): MSCNN. (f): NLD. (g): VRHI. (h): Ground truth.

it will supersaturate the details in dark regions. As shown Fig. 6(e), MSCNN is able to produce the haze-free results when dealing with some mist images, while it fails to uncover the details for the scenes with dense haze. From Fig. 6(f), we can observe that NLD suffers from color distortion and lacks the ability to deal with the scenes with gray white colors trend. In comparison, VRHI shows the best dehazing performance, while avoiding any visually negative effects as demonstrated in Fig. 6(g).

5. Conclusion

In this paper, a haze density model is designed to estimate the haze distribution of an image. Based on this model and atmospheric scattering model, a hazy image restoration method called VRHI is developed. Unlike other dehazing techniques, a novel strategy of using whole image is utilized to estimate the transmission map and recursively refine the atmospheric light, which enables VRHI to avoid negative visual effects, e.g., color distortion and detail over-enhancement. Moreover, without any refining process or training process, high-quality restored images can be obtained from the proposed VRHI. A series of experimental results verify VRHI has the capability for robust utilization and accurate restoration, which outperforms most state-of-the-art techniques.

6. Acknowledgement

This work was supported by National Natural Science Foundation of China (61902198), Natural Science Foundation of Jiangsu Province (BK20190730), Research Fund of Nanjing University of Posts and Telecommunications (NY219135), and in part by Key Laboratory of Radar Imaging and Microwave Photonics, Ministry of Education, for Nanjing University of Aeronautics and Astronautics.

References

[1] Y. Bahat and M. Irani. Blind dehazing using internal patch recurrence. In *2016 IEEE International Conference on Computational Photography (ICCP)*, pages 1–9, 2016. 1, 4

[2] D. Berman, T. Treibitz, and S. Avidan. Non-local image dehazing. In *2016 IEEE Conference on Computer Vision and Pattern Recognition (CVPR)*, pages 1674–1682, 2016. 1, 4

[3] D. Berman, T. Treibitz, and S. Avidan. Single image dehazing using haze-lines. *IEEE Transactions on Pattern Analysis and Machine Intelligence*, 42(3):720–734, 2020. 1

[4] N. Bharath Raj and N. Venketeswaran. Single image haze removal using a generative adversarial network. In *2020 International Conference on Wireless Communications Signal Processing and Networking (WiSPNET)*, pages 37–42, 2020. 2

[5] T. M. Bui and W. Kim. Single image dehazing using color ellipsoid prior. *IEEE Transactions on Image Processing*, 27(2):999–1009, 2018. 1

[6] B. Cai, X. Xu, K. Jia, C. Qing, and D. Tao. Dehazenet: An end-to-end system for single image haze removal. *IEEE Transactions on Image Processing*, 25(11):5187–5198, 2016. 1

[7] L. K. Choi, J. You, and A. C. Bovik. Referenceless prediction of perceptual fog density and perceptual image defogging. *IEEE Transactions on Image Processing*, 24(11):3888–3901, 2015. 1, 4

[8] S. D. Das and S. Dutta. Fast deep multi-patch hierarchical network for nonhomogeneous image dehazing. In *2020 IEEE/CVF Conference on Computer Vision and Pattern Recognition Workshops (CVPRW)*, pages 1994–2001, 2020. 1

[9] H. Dong, J. Pan, L. Xiang, Z. Hu, X. Zhang, F. Wang, and M. H. Yang. Multi-scale boosted dehazing network with dense feature fusion. In *2020 IEEE/CVF Conference on Computer Vision and Pattern Recognition (CVPR)*, pages 2154–2164, 2020. 4

[10] A. Dudhane, H. S. Aulakh, and S. Murala. Ri-gan: An end-to-end network for single image haze removal. In *2019 IEEE/CVF Conference on Computer Vision and Pattern Recognition Workshops (CVPRW)*, pages 2014–2023, 2019. 2

[11] A. Dudhane and S. Murala. Cdnet: Single image de-hazing using unpaired adversarial training. In *2019 IEEE Winter Conference on Applications of Computer Vision (WACV)*, pages 1147–1155, 2019. 2

[12] A. Dudhane and S. Murala. Ryf-net: Deep fusion network for single image haze removal. *IEEE Transactions on Image Processing*, 29:628–640, 2020. 1

[13] D. Engin, A. Genc, and H. K. Ekenel. Cycle-dehaze: Enhanced cyclegan for single image dehazing. In *2018 IEEE/CVF Conference on Computer Vision and Pattern Recognition Workshops (CVPRW)*, pages 938–9388, 2018. 2

[14] Y. Gao, H. Hu, B. Li, Q. Guo, and S. Pu. Detail preserved single image dehazing algorithm based on airlight refinement. *IEEE Transactions on Multimedia*, 21(2):351–362, 2019. 1

[15] K. He, J. Sun, and X. Tang. Single image haze removal using dark channel prior. *IEEE Transactions on Pattern Analysis and Machine Intelligence*, 33(12):2341–2353, 2011. 1, 4

[16] L. He, J. Zhao, N. Zheng, and D. Bi. Haze removal using the difference- structure-preservation prior. *IEEE Transactions on Image Processing*, 26(3):1063–1075, 2017. 1

[17] S. Huang, J. Ye, and B. Chen. An advanced single-image visibility restoration algorithm for real-world hazy scenes. *IEEE Transactions on Industrial Electronics*, 62(5):2962–2972, 2015. 1

[18] X. Jin, Z. Chen, J. Lin, W. Zhou, J. Chen, and C. Shan. Ai-gan: Signal de-interference via asynchronous interactive generative adversarial network. In *2019 IEEE International Conference on Multimedia Expo Workshops (ICMEW)*, pages 228–233, 2019. 2

[19] A. Jolfaei and K. Kant. Privacy and security of connected vehicles in intelligent transportation system. In *2019 49th Annual IEEE/IFIP International Conference on Dependable Systems and Networks Supplemental Volume (DSN-S)*, pages 9–10, 2019. 1

[20] M. Ju, C. Ding, and Y. J. Guo. Vrohi: Visibility recovery for outdoor hazy image in scattering media. *IEEE Photonics Journal*, 12(6):1–15, 2020. 1

[21] M. Ju, C. Ding, Y. J. Guo, and D. Zhang. Remote sensing image haze removal using gamma-correction-based dehazing model. *IEEE Access*, 7:5250–5261, 2019. 1

[22] M. Ju, C. Ding, Y. J. Guo, and D. Zhang. Idgcp: Image dehazing based on gamma correction prior. *IEEE Transactions on Image Processing*, 29:3104–3118, 2020. 1

[23] M. Ju, C. Ding, W. Ren, Y. Yang, D. Zhang, and Y. J. Guo. Ide: Image dehazing and exposure using an enhanced atmospheric scattering model. *IEEE Transactions on Image Processing*, 30:2180–2192, 2021. 1

[24] M. Ju, C. Ding, D. Zhang, and Y. J. Guo. Gamma-correction-based visibility restoration for single hazy images. *IEEE Signal Processing Letters*, 25(7):1084–1088, 2018. 1

[25] M. Ju, C. Ding, D. Zhang, and Y. J. Guo. Bdpk: Bayesian dehazing using prior knowledge. *IEEE Transactions on Circuits and Systems for Video Technology*, 29(8):2349–2362, 2019. 1

[26] B. Li, X. Peng, Z. Wang, J. Xu, and D. Feng. Aod-net: All-in-one dehazing network. In *2017 IEEE International Conference on Computer Vision (ICCV)*, pages 4780–4788, 2017. 1

[27] B. Li, W. Ren, D. Fu, D. Tao, D. Feng, W. Zeng, and Z. Wang. Benchmarking single-image dehazing and beyond. *IEEE Transactions on Image Processing*, 28(1):492–505, 2019. 5

[28] L. Li, Y. Dong, W. Ren, J. Pan, C. Gao, N. Sang, and M. H. Yang. Semi-supervised image dehazing. *IEEE Transactions on Image Processing*, 29:2766–2779, 2020. 1

[29] R. Li, J. Pan, Z. Li, and J. Tang. Single image dehazing via conditional generative adversarial network. In *2018 IEEE/CVF Conference on Computer Vision and Pattern Recognition*, pages 8202–8211, 2018. 2

[30] P. Liu, S. Horng, J. Lin, and T. Li. Contrast in haze removal: Configurable contrast enhancement model based on dark channel prior. *IEEE Transactions on Image Processing*, 28(5):2212–2227, 2019. 1

[31] X. Liu, Y. Ma, Z. Shi, and J. Chen. Griddehazenet: Attention-based multi-scale network for image dehazing. In *2019 IEEE/CVF International Conference on Computer Vision (ICCV)*, pages 7313–7322, 2019. 1

[32] Y. Liu, J. Pan, J. Ren, and Z. Su. Learning deep priors for image dehazing. In *2019 IEEE/CVF International Conference on Computer Vision (ICCV)*, pages 2492–2500, 2019. 1

[33] A. Mehta, H. Sinha, P. Narang, and M. Mandal. Hidegan: A hyperspectral-guided image dehazing gan. In *2020 IEEE/CVF Conference on Computer Vision and Pattern Recognition Workshops (CVPRW)*, pages 846–856, 2020. 2

[34] G. Meng, Y. Wang, J. Duan, S. Xiang, and C. Pan. Efficient image dehazing with boundary constraint and contextual regularization. In *2013 IEEE International Conference on Computer Vision*, pages 617–624, 2013. 4

[35] J. Pan, J. Dong, Y. Liu, J. Zhang, J. Ren, J. Tang, Y. W. Tai, and M. H. Yang. Physics-based generative adversarial models for image restoration and beyond. *IEEE Transactions on*

Pattern Analysis and Machine Intelligence, pages 1–1, 2020. 2

[36] D. Park, H. Park, D. K. Han, and H. Ko. Single image dehazing with image entropy and information fidelity. In *2014 IEEE International Conference on Image Processing (ICIP)*, pages 4037–4041, 2014. 3

[37] J. Park, D. K. Han, and H. Ko. Fusion of heterogeneous adversarial networks for single image dehazing. *IEEE Transactions on Image Processing*, 29:4721–4732, 2020. 2

[38] Y. Peng, Z. Lu, F. Cheng, Y. Zheng, and S. Huang. Image haze removal using airlight white correction, local light filter, and aerial perspective prior. *IEEE Transactions on Circuits and Systems for Video Technology*, 30(5):1385–1395, 2020. 2, 3

[39] Y. Qu, Y. Chen, J. Huang, and Y. Xie. Enhanced pix2pix dehazing network. In *2019 IEEE/CVF Conference on Computer Vision and Pattern Recognition (CVPR)*, pages 8152–8160, 2019. 2, 4

[40] W. Ren, S. Liu, L. Ma, Q. Xu, X. Xu, X. Cao, J. Du, and M. Yang. Low-light image enhancement via a deep hybrid network. *IEEE Transactions on Image Processing*, 28(9):4364–4375, 2019. 1

[41] Wenqi Ren, Si Liu, Hua Zhang, Jinshan Pan, Xiaochun Cao, and Ming-Hsuan Yang. Single image dehazing via multi-scale convolutional neural networks. In Bastian Leibe, Jiri Matas, Nicu Sebe, and Max Welling, editors, *Computer Vision – ECCV 2016*, pages 154–169, Cham, 2016. Springer International Publishing. 1, 4

[42] W. Ren, J. Yang, S. Deng, D. Wipf, X. Cao, and X. Tong. Face video deblurring using 3d facial priors. In *2019 IEEE/CVF International Conference on Computer Vision (ICCV)*, pages 9387–9396, 2019. 1

[43] W. Ren, J. Zhang, J. Pan, S. Liu, J. Ren, J. Du, X. Cao, and M. H. Yang. Deblurring dynamic scenes via spatially varying recurrent neural networks. *IEEE Transactions on Pattern Analysis and Machine Intelligence*, pages 1–1, 2021. 1

[44] W. Ren, J. Zhang, X. Xu, L. Ma, X. Cao, G. Meng, and W. Liu. Deep video dehazing with semantic segmentation. *IEEE Transactions on Image Processing*, 28(4):1895–1908, 2019. 1

[45] J. Shen, Z. Li, L. Yu, G. Xia, and W. Yang. Implicit euler ode networks for single-image dehazing. In *2020 IEEE/CVF Conference on Computer Vision and Pattern Recognition Workshops (CVPRW)*, pages 877–886, 2020. 1

[46] H. Sim, S. Ki, J. Choi, S. Y. Kim, S. Seo, S. Kim, and M. Kim. High-resolution image dehazing with respect to training losses and receptive field sizes. In *2018 IEEE/CVF Conference on Computer Vision and Pattern Recognition Workshops (CVPRW)*, pages 1025–10257, 2018. 2

[47] Y. Song, J. Li, X. Wang, and X. Chen. Single image dehazing using ranking convolutional neural network. *IEEE Transactions on Multimedia*, 20(6):1548–1560, 2018. 1

[48] R. T. Tan. Visibility in bad weather from a single image. In *2008 IEEE Conference on Computer Vision and Pattern Recognition*, pages 1–8, 2008. 1

[49] A. Wang, W. Wang, J. Liu, and N. Gu. Aipnet: Image-to-image single image dehazing with atmospheric illumination prior. *IEEE Transactions on Image Processing*, 28(1):381–393, 2019. 1

[50] W. Wang, X. Yuan, X. Wu, and Y. Liu. Fast image dehazing method based on linear transformation. *IEEE Transactions on Multimedia*, 19(6):1142–1155, 2017. 1

[51] X. Wang, M. Ju, and D. Zhang. Image haze removal via a multiscale fusion and total variation. *Journal of Systems Engineering and Electronics*, 28(3):597–605, 2017. 1

[52] Y. Yan, S. Zhang, M. Ju, W. Ren, R. Wang, and Y. Guo. A point light source interference removal method for image dehazing. In *2020 IEEE/CVF Conference on Computer Vision and Pattern Recognition Workshops (CVPRW)*, pages 3817–3825, 2020. 1

[53] M. Yang, J. Liu, and Z. Li. Superpixel-based single nighttime image haze removal. *IEEE Transactions on Multimedia*, 20(11):3008–3018, 2018. 1

[54] X. Zhang, T. Wang, W. Luo, and P. Huang. Multi-level fusion and attention-guided cnn for image dehazing. *IEEE Transactions on Circuits and Systems for Video Technology*, pages 1–1, 2020. 1

[55] H. Zhu, Y. Cheng, X. Peng, J. T. Zhou, Z. Kang, S. Lu, Z. Fang, L. Li, and J. H. Lim. Single-image dehazing via compositional adversarial network. *IEEE Transactions on Cybernetics*, 51(2):829–838, 2021. 2

[56] Q. Zhu, J. Mai, and L. Shao. A fast single image haze removal algorithm using color attenuation prior. *IEEE Transactions on Image Processing*, 24(11):3522–3533, 2015. 1